

MODELING THE BEHAVIOR OF SELECTED WATER-SOLUBLE ELEMENTS IN CALCIUM SULFATE VEINS OF GALE CRATER. D. Das¹, P. J. Gasda², S. P. Schwenzer³, L. Crossey⁴, S. M. R. Turner³, R. J. Leveille¹, K. Berlo¹, R. C. Wiens² ¹Department of Earth and Planetary Sciences, McGill University, Quebec, Canada (debarati.das@mail.mcgill.ca), ²Los Alamos National Laboratory, New Mexico, USA, ³AstrobiologyOU, The Open University, Milton Keynes, United Kingdom, ⁴University of New Mexico, New Mexico, USA.

Introduction: From late 2017 to early 2019, the NASA *Curiosity* rover crossed a morphologically resistant feature in Gale crater named Vera Rubin ridge (VRR). VRR is a ~200 m wide and ~6.5 km long ridge that is inferred to have formed due to preferential hardening caused by late-stage diagenetic processes such as enhanced crystallization and/or cementation [1]. The rover's ChemCam instrument suite detected water-soluble elements B and Li in Ca-sulfate veins throughout VRR [2]. ChemCam has made similar detections in Gale crater prior to arriving at VRR [3]. Due to the overall high solubilities of B and Li relative to Ca-sulfate and the difference in relative solubilities between the two elements, their abundances can be a marker of progressing evaporation of Gale crater fluids and improve the understanding of the crater's late-stage diagenetic events [2].

Ca-sulfates of Gale crater contain relatively high amounts of B and Li (highest concentration of B and Li respectively observed in Gale crater: ~300 and 65 ppm [2, 3]) compared to Ca-sulfates or basalts on Earth (Ca-sulfates: <20 ppm B [4], < 7 ppm Li [5]; basalts: <20 ppm B [6], <30 ppm Li [6]). The B and Li abundances in Ca-sulfate veins of Gale crater also show a broad inverse correlation between them (especially in VRR) [2].

We hypothesized that the enrichment of B and Li was caused by progressive dehydration of late-stage diagenetic fluids and the relationship between B and Li is a result of a combination of processes such as sequential evaporation (B precipitating as salts faster than Li due to B's solubility which is about ten times lower than Li in water at 1atm and 20°C [7]), adsorption to clays, and/or remobilization of B and Li after clay dissolution in an acidic fluid environment [2]. The hypothesis is based on the presence of crystalline akaganeite and jarosite indicating acidic and warm fluids [1, 8] and lower Li abundance in VRR [9], in addition to the observed B and Li concentrations. Elevated Li and clay content below VRR is also inferred to indicate an impermeable layer [9] which could mean that B and Li in VRR may have been sourced locally or upslope (i.e., due to dissolution of clays). To summarize, we hypothesized that adsorption, dissolution, sequential evaporation, and possibly multiple generations of dissolution and re-precipitation caused the enrichment and the broad inverse correlation of B and Li in Ca-sulfates of VRR and that

the B and Li were locally sourced [2]. However, the relationship between B and Li abundances in Gale Ca-sulfates is not an exact correlation and not all targets show this trend [2]. Hence, we surmised that geochemical modeling would be required to confirm our hypothesis and to what additional processes may have occurred to produce the observed data.

We aim to understand the processes and the sequence of events using a combination of analog sample investigations and reaction-pathway modeling of the terrestrial situation, followed by extrapolation to Mars. We focus on analog samples from Death Valley, USA [10], published results of evaporites and groundwater around dry lakes of Death Valley [11] and Valles Caldera [12] in USA, ground and spring water from Iceland [6], and evaporites and ground water from dry lakes of Bolivia [13]. In this abstract we will focus on the methodology developed for geochemical modeling of low-temperature (<100°C) fluids in an evaporative setting to understand the reasons behind enrichment of B and Li after adding the relevant B and Li phase thermochemical data to the existing model databases.

Methodology: As Li and B phases observed in our analogs and their thermochemical constants are not currently included in geochemical models, we start by expanding the thermochemical database from the literature [14, 15]. Thermochemical modeling is performed using Gibbs free energy calculations between chosen starting materials using CHIM-XPT. CHIM-XPT [16] is a program for computing equilibria between multiple components in aqueous-mineral-gas systems and will be used for the initial thermochemical modeling. Geochemist's Workbench [17] will be used to further refine the model and include processes such as adsorption of B and Li to clays. The modeling process is divided into three stages which iteratively increase in complexity with respect to geological processes as shown in Fig 1a. Stage 1 in Fig 1a shows that the model will start by composing a fluid that has reached equilibration with Gale crater rocks (e.g. in 1 liter of water with ions: Ca²⁺, SO₄²⁻, Na⁺, Cl⁻, B(OH)₄⁻ and Li⁺). Evaporation and dissolution for this fluid will then be modeled using CHIM-XPT. The resultant phases (both fluid and precipitates) will be used as starting materials for a second stage of the modeling process. The final stage will take into

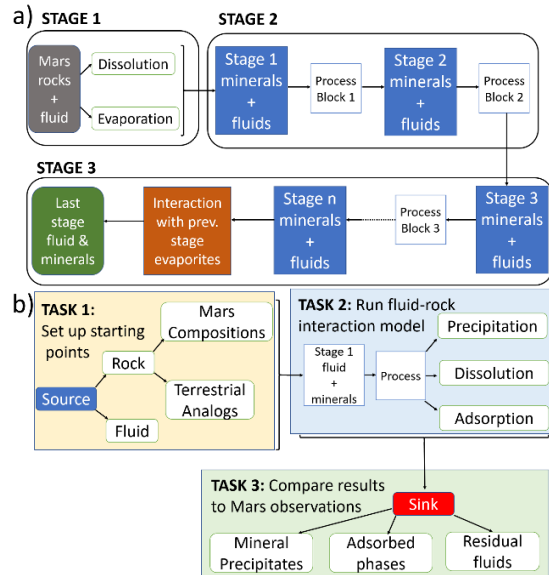


Figure 1. a) Three stages of thermochemical modeling. Process block indicates possible sets of geological events such as precipitation, dissolution and adsorption. b) Task sets in each thermochemical modeling stage shown in a).

consideration multiple events such as precipitation, dissolution, adsorption and intergenerational interaction of fluids and precipitates. Each stage will consist of three sets of tasks as shown in Fig 1 b). The first task will consist of setting up the starting materials for the model, the second task will consist of simulating evaporation and dissolution using CHIM-XPT, and the third task will consist of comparing the resultant phases to Mars observations and terrestrial analogs. With each stage we will iteratively increase the complexity of the model by simulating evaporation, dilution, and by adjusting the ionic composition of the starting fluid based on the comparisons with Mars observations and terrestrial analogs. The first stage of the modeling process will focus on the broad understanding of the composition, temperature, pH, and water-rock ratio of fluids that formed primary (or first generation) evaporites in Gale crater. The second stage will focus on determining the parameters of fluids that formed Ca-sulfates in Gale crater [18] and the final stage will refine the model to understand what fluids formed the veins in VRR [2]. At each stage we will test the model using a terrestrial analog (for which we have published mineral, brine, and groundwater compositional data) using the model to establish a ground truthing. The terrestrial analogs are chosen based on similarity to conditions in Gale crater and the availability of relevant data (trace and major element concentrations of varying lithologies, stream and ground water data, etc.). For example, Iceland is a promising candidate due to the extensive availability of rock [6], stream [19, 20] and ground-water [21] data.

Preliminary Results: CHIM-XPT was used to evaporate 1 L of fluid containing Ca^{2+} (200 ppm), SO_4^{2-} (200 ppm), Cl^- (200 ppm), Na^+ (100 ppm), and Li^+ (100 ppm) over 1-60°C. The resultant phase abundances with varying H_2O content is shown in Fig 2. With decreasing water content phases NaCl, LiCl, CaCl_2 form more readily than CaSO_4 , gypsum and anhydrite (Fig 2 inset).

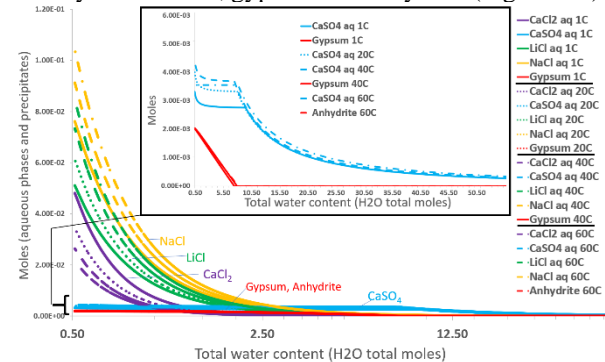


Figure 2. Resultant aqueous and precipitated phases (y-axis) plotted v/s total H_2O in the solution (x-axis shown in log scale). Inset shows CaSO_4 , gypsum, and anhydrite on a linear scale for x-axis.

Future Work: Common B phase thermochemical data are yet to be added to the CHIM-XPT database. On addition of the thermochemical data, refining the starting fluid composition and temperature range the resultant mineral species are expected to include borate salts (such as: inyoite, ulexite, kernite and borax for neutral to high pH, low-temperature environments; colemanite for neutral to high pH, high-temperature environments, and sassolite for low pH, low-temperature environments [3, 22, 23]), providing an insight about the initial B content of Gale diagenetic fluids. With increasing number of iterative steps of the model, the resultant phases and reaction pathways are expected evolve to a closer approximation of the late-stage diagenetic events of Gale crater.

Acknowledgement: NSERC Discovery prog., CSA support for NASA MSL Participating Scientists, LANL, UKSA Aurora.

References: [1] Fraeman et al., (2020) *JGR:P*; [2] Das et al., (2020) *JGR:P*; [3] Gasda et al., (2017) *GRL*; [4] Ma et al., (2017) *Tnta*. 175, 250-255; [5] Dutrizac et al., (2017) *Hydromet*. 174, 38-46; [6] Lacasse et al., *BOV* 64.4, 373; [7] Dalton et al., (2016) *NIST Sol. DB*; [8] Rampe et al., (2020) *JGR:P*; [9] Frydenvang et al., (2020) *JGR:P*; [10] Das et al., (2020) *LPI* 2326, 1080; [11] Janick et al., (2019), *JOP*, 62.1, 105-120; [12] Goff et al., (2002) *JVGR* 116, 299-323; [13] Haferburg et al., (2017) *Microb. Res.* 199, 19-28; [14] Anovitz et al., (1996) *RIM* 33,181-222; [15] Monnin et al., (2002) *JCED* 47.6, 1331-1336; [16] Reed et al., (2010) *U. Oregon*; [17] Bethke et al., (2007) *U. Illinois*; [18] Nachon et al., (2017) *Icarus* 281, 121-136; [19] Ólafsson et al., (1978) *Chem. Geo* 21.3, 4; [20] Arnórsson et al., (1995) *GCA* 59.20, 4125-4146; [21] Giroud et al., (2008) *U. Iceland*; [22] Christ et al., (1967) *GCA*, 31.3, 313-337; [23] Birsoy et al., (2012) *CAE*, 27.1, 71-85.